Chapter 32

Thermo-mechanical Design of a Compact X-ray Target of Dual Energy LINAC

– *Kumar Sajal, R. Barnwal & S. R. Ghodke*

The 6 MeV/ 4 MeV dual energy Linear Accelerator (LINAC) developed at Electron Beam Center (EBC), Navi Mumbai produces X-Ray for the purpose of cargo-scanning, radiography and irradiation. The accelerator consists of an electron gun which produces pulsed electron beam, an RF cavity which is an on-axis coupled cavity standing wave structure having accelerating cavities along with coupling cavities, a focusing magnet and a compact X-Ray target assembly. X-ray is produced by bombardment of high energy electrons on thin tungsten disc in target assembly by the process of bremsstrahlung. The choice of tungsten as desired target material is because of its high atomic number leading to high interaction of electrons with material as well as very high melting point (3422 °C). The thickness of the tungsten disc has been optimized as lower thickness results is lower interaction of electron beam with target material hence lower conversion into X-Ray while higher thickness results in self-attenuation of X-ray hence less output. The optimum thickness of the tungsten disc has been evaluated in EBC by GEANT4 Monte Carlo code which has been developed by CERN and comes out to be 1.2 mm for 6 MeV electron beam energy. The LINAC is operated in a high vacuum environment at 120 mA pulsed beam current for 6 MeV beam energy with Pulse Width (PW) of 4 μs and Pulse Repetition Frequency (PRF) of 200 Hz. The power of the electron beam can be evaluated by multiplying voltage (through which the electron is accelerated) with beam current, PW and PRF, which comes out to be 576 W. A large part of this beam power ($\sim$76%) is deposited as thermal power in tungsten disc which has been evaluated in EBC in FLUKA Monte Carlo Code developed by CERN. The target assembly has been prepared by brazing of tungsten disc with SS316L CF-35 con-flat flange. The deposition of such high thermal power in the thin tungsten disc gives rise to various design challenges which is discussed in subsequent section. A high vacuum of 10^{-6} mbar or better is required for operation of the accelerator. The brazing joint in the target assembly is the barrier between high vacuum inside LINAC and high-pressure cooling water flowing over the target material. The brazing joint also suffers high irradiation doses due to which the copper in filler material loose ductility and develops crack due to thermal cycling. The design of target hence requires careful examination of temperature and stress distribution in brazing joint at various cooling water flow rates so as to maximize its service life.

32.1 Design Challenges

The major design challenges and their solutions are discussed below:

a. There is necessity of joining dissimilar materials. Brazing is done for joining SS316L con-flat flange with thin tungsten disc using copper-silver eutectic alloy (72% silver and 28% copper) filler material.

b. The thermal power deposited on thin tungsten disc is very high ($\sim$440 W). This may lead to high temperature of brazing joint which should be investigated carefully as the melting point of eutectic filler materials is 780 °C. High temperature in brazing joint also introduces high stresses in it due to dissimilar thermal expansion coefficients of tungsten (4.4×10^{-6} /K) and stainless steel (16×10^{-6} /K). To protect the brazing joint from very high temperature and stresses, a very high rate of heat extraction mechanism has to be adopted. This has been achieved by flowing cooling water directly over the tungsten disc as can be seen in Fig. 32.1.

c. For generating sufficient convective heat transfer rate over the tungsten disc and nearby heated zones, certain flow rates are required. This has been achieved by providing 6-8 bar operating pressure of cooling water. This high pressure of cooling water should not further put stress on the brazing joint. This has been achieved by making step on stainless steel flange and tungsten disc and resting the disc against the step of flange.

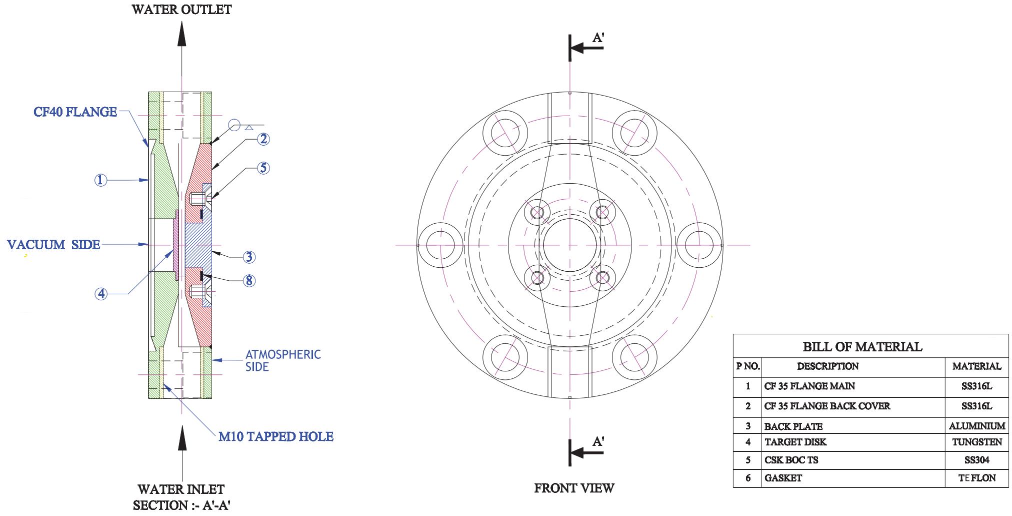

BILL OF MATERIAL

P NO.	DESCRIPTION	MATERIAL
1	CF 35 FLANGE MAIN	SS316L
2	CF 35 FLANGE BACK COVER	SS316L
3	BACK PLATE	ALUMINIUM
4	TARGET DISK	TUNGSTEN
5	CSK BOC TS	SS304
6	GASKET	TE FLON

Figure 32.1: 2-D Drawing of Target Assembly.

The high pressure cooling water flows on atmospheric side of the disc such that the high pressure of cooling water further presses the disc against the flange.

d. To provide access to brazing on water wetted joint between tungsten and SS, the conflat flange is made in two parts. The part no. 2 (refer Fig. 32.1) is made of same SS316L material and is welded to the part no. 1 after brazing is completed.

e. The electrons which are transmitted through the tungsten disc need to be attenuated as it might interfere with our intended operation. A back plate of aluminum (part no. 3 in Fig. 32.1) of thickness 6 mm is provided. It is fitted with the help of Teflon gasket (part no. 6 in Fig. 32.1) in and SS 304 CSK bolts (part no. 3 in Fig. 32.1).

f. The brazing joint suffers high irradiation dose of ∼1 MGy/hour during the operation of accelerator. There is a loss of ductility of copper in filler material after cumulative dose of 80 MGy [153]. The thermal cycling in the resulting brittle material causes microcracks which further aggravated by the high-pressure cooling water flowing over it. It has been observed that the vacuum inside the accelerator starts degrading after 80-100 hours of operation of accelerator when a leak rate of 10^{-7} mbar l/s is measured in the brazing joint. A detailed thermal and structural analysis has been performed to estimate the required flow rate to limit the temperature and stresses in the brazing joint.

32.2 Thermal and Structural Analysis

The thermal coupled structural analysis has been performed in FEM module of ANSYS workbench. A 3-D model has been prepared (Fig. 32.2) for this purpose. Meshing has been performed for the analysis using Finite Element Method. The maximum edge length in any tetrahedral grid is less than or equal to 0.5 mm. The meshing size has been checked for grid independence for all the evaluated results. Figure 32.3 shows the meshing of the complete target assembly. The material properties of individual parts have been provided in the FEM analysis. A heat load of 440 W deposited uniformly in the tungsten disc material is provided to the analysis. Convective heat transfer coefficients have been evaluated in different zones

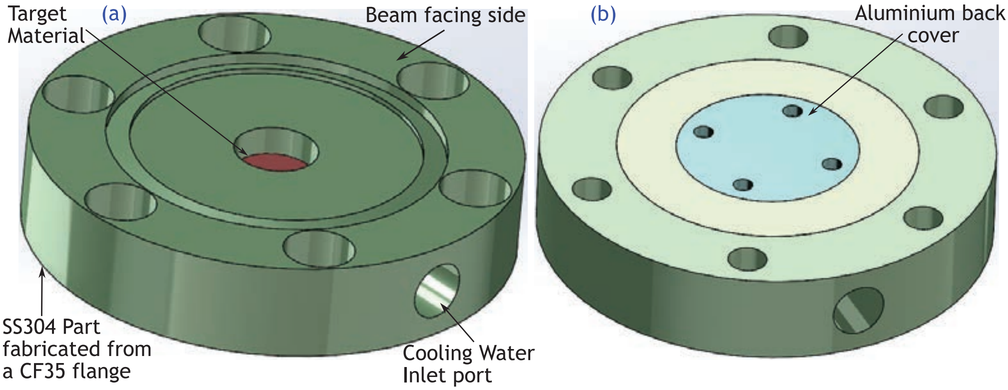

Figure 32.2: 3-D model of the target assembly: (a) vacuum side face, and (b) atmospheric side face.

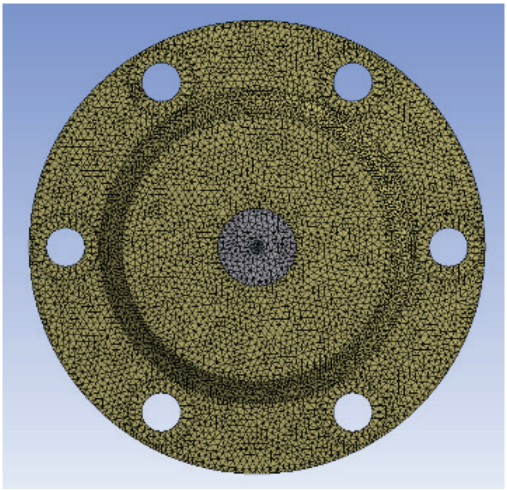

Figure 32.3: Meshing of the target assembly using tetrahedral meshes.

(Fig. 32.4) separately where cooling water is flowing and has been provided to the analysis. Nusselt number correlation given by Gnielinski, valid for (a) transient & turbulent regions (b) thermally underdeveloped flow and (c) large temperature difference between wall and fluid has been utilized for evaluation of convective heat transfer coefficients [154].

$$N_u = \frac{\left(\frac{f}{8}\right)(R_e - 1000)P_r}{1 + 12.7\left(\frac{f}{8}\right)^{0.5}(P_r^{\frac{2}{3}} - 1)}\left[1 + \left(\frac{D}{l}\right)^{\frac{2}{3}}\right]\left(\frac{P_{rm}}{P_{rw}}\right)^{0.11} \tag{32.1}$$

where, Darcy friction factor, $f = (0.79 \log_e R_e - 1.64)^{-2}$ can be calculated from Petukhov explicit correlation valid for $3000 < \mathrm{R}_e < 5000000$ [155].

The temperatures are evaluated in Finite Element Method (FEM) module of ANSYS workbench. The steady state temperature results are given as input to structural analysis along with cooling water design pressure value of 10 bar and structural restraints. The structural analysis is further performed and stress distributions are evaluated in the assembly.

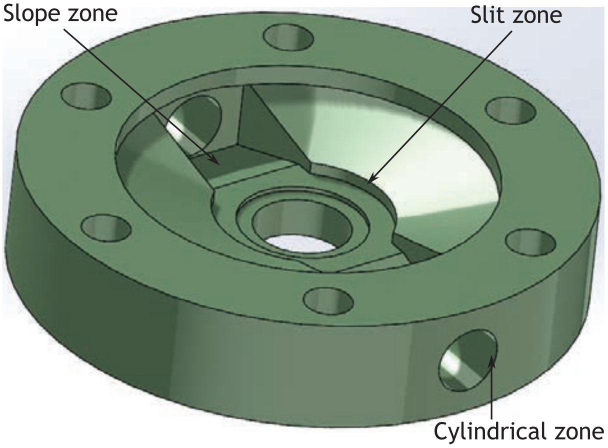

Figure 32.4: Different zones in cooling water flow path for the purpose of evaluation of convective heat transfer coefficient.

Table 32.1: Evaluation of convective heat transfer coefficients in the slit zone at different flow rates.

Flow Rate (F) LPM	Velocity (v) m/s	Reynolds No. (R_e)	Darcy friction factor (f)	Nusselt's No. (N_u)	Heat transfer coefficient (h) W/m^2K
1	0.61	1911	0.053	8.39	1802
3	1.84	5732	0.037	71.74	15404
5	3.07	9553	0.031	117.48	25226
8	4.91	15285	0.028	180.08	38669
10	6.14	19106	0.026	219.49	47130

32.3 Results

The temperature and stress distribution in the brazing joint as well as the complete assembly is being investigated at different flow rates to ensure safety of the joint.

Table 32.2: Peak temperature in Target Assembly and Brazing Joint at different flow rate.

S.No.	Cooling Water Flow Rate (LPM)	Peak Temperature in Target Assembly (℃)	Peak Temperature in Brazing Joint (℃)
1	1	1134	481
2	3	644	99
3	5	572	67
4	8	516	49
5	10	492	43

Table 32.3: Peak Stress in Target Assembly and Brazing Joint at different flow rates.

S.No.	Cooling Water Flow Rate (LPM)	Peak Stress in Target Assembly (MPa)	Peak Stress in Brazing Joint (MPa)
1	1	3550	1223
2	3	554	207
3	5	484	136
4	8	431	97
5	10	409	84

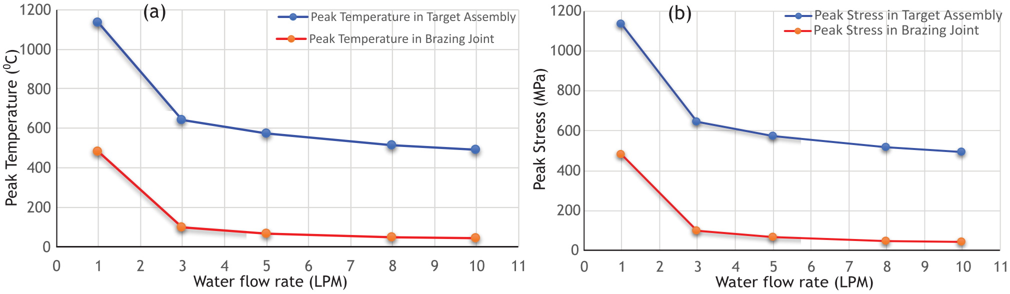

Figure 32.5: Investigations at different flow rates for brazing joint and complete target assembly: (a) peak temperature distribution, and (b) peak stress distribution.

32.4 Conclusion

The peak temperature and peak stress distributions in the complete assembly have been studied (Fig. 32.5). The brazing joint is the most critical zone in the target assembly. It is a copper-silver eutectic alloy (72% Ag and 28% Cu) with melting point of 780 °C. From Table 32.2, we can see that at all flow rates ranging from 1 LPM to 10 LPM, the peak temperature in the brazing joint does not even reach the half of the melting point, hence safe when temperature is concerned. The yield strength of copper-silver alloy is 282 MPa and ultimate tensile strength is 382 MPa while the allowable stress can be evaluated as 182 MPa when factor of safety is taken as 1.5. From Table 32.3, we can see that the brazing joint is safe from any structural failure at flow rates 5 LPM and above. Hence, 5 LPM can be chosen as safe cooling water flow rate when radiation damages are not taken into the account. To solve the problem of reduced ductility of copper in joint due to irradiation we have looked into alternate methods of joint preparation. We have designed a new target assembly in which stainless steel flange and tungsten disc joining will be done by electron beam welding method. The results will be discussed in subsequent publications.